Three Conserved Guanosines Approach the Reaction Site in Native and Minimal Hammerhead Ribozymes†

Dominic Lambert, Joyce E. Heckman, and John M. Burke*

Department of Microbiology and Molecular Genetics, University of Vermont, 95 Carrigan Drive, 220B Stafford Hall, Burlington, Vermont 05405

Received December 1, 2005; Revised Manuscript Received April 7, 2006

ABSTRACT: Native hammerhead ribozymes contain RNA domains that enable high catalytic activity under physiological conditions, where minimal hammerheads show little activity. However, little is known about potential differences in native versus minimal ribozyme folding. Here, we present results of photocrosslinking analysis of native and minimal hammerheads containing photoreactive nucleobases 6-thioguanosine, 2,6-diaminopurine, 4-thiouridine, and pyrrolocytidine, introduced at specific sites within the catalytic core. Under conditions where catalytic activity is observed, the two substrate nucleobases spanning the cleavage site approach and stack upon G8 and G12 of the native hammerhead, two conserved nucleobases that show similar behavior in minimal constructs, have been implicated in general acid−base catalysis, and are >15 Å from the cleavage site in the crystal structures. Pyrrolocytidine at cleavage site position 17 forms an efficient crosslink to G12, and the crosslinked RNA retains catalytic activity. Multiple crosslinked species point to a structural rearrangement within the U-turn, positioning residue G5 in the vicinity of cleavage site position 1.1. Intriguing crosslinks were triggered by nucleotide analogues at positions distal to the crosslinked residues; for example, 6-thioguanosine at position 5 induced a crosslink between G12 and C17, suggesting an intimate functional communication among these three nucleobases. Together, these results support a model in which the native hammerhead folds to an active structure similar to that of the minimal ribozyme, and significantly different from the crystallographic structures.

The hammerhead is a small catalytic RNA that carries out the reversible cleavage of a phosphodiester bond, creating 2′,3′-cyclic phosphate and 5′-hydroxyl termini. Crystal structures of the hammerhead display a Y-shaped structure in which the scissile linkage is not arranged appropriately for an in-line attack (*1*, *2*). This clearly necessitates a conformational change for catalysis, but disagreement exists concerning the scale of the structural rearrangement. Scott and co-workers propose that a small-scale local rearrangement occurs around the scissile linkage and that reaction chemistry depends primarily upon the proper alignment of attacking, phosphate, and leaving groups (*3*, *4*). However, studies of the relationship between geometry and stability of internucleotide linkages suggest that an ideal geometry for in-line attack can account for at most a rate acceleration of 10^2-fold over the uncatalyzed reaction, compared to the $\sim 10^7$-fold of the hammerhead cleavage (*5*). Originally thought to be Mg^{2+}-dependent, the hammerhead reaction functions in the presence of high concentrations of monovalent cations or $[Co(NH_3)_6]^{3+}$, indicating that inner-sphere coordination of metal ions is not required for activity (*6*, *7*). An alternative explanation is that the ribozyme uses different mechanisms in solutions containing monovalent versus divalent cations (*8*).

The crystal structure is not consistent with a large quantity of biochemical data, and these inconsistencies have been used as the basis for a hypothesis that a large-scale conformational rearrangement is required for catalysis (*9*). A single Mg^{2+} ion bridges the pro-R oxygen of the scissile phosphate and the pro-R oxygen of residue A9 in domain II, located some 20 Å apart in the crystal structure (*10*, *11*). Important functional groups of G5, G8, and G12 form no contacts in the crystal structure (*12*), and bulky substituents introduced at specific 2′ positions are strongly inhibitory, even though they can be readily accommodated within the crystal structure (*13*). Backbone protection results suggest that the predominant structure in solution resembles the crystal structure; however, significantly higher cation concentrations are required for catalysis than for accessing this predominant fold (*14*). Thus, the active structure of the ribozyme, however different it may be from the inactive basic fold, may be accessed only transiently.

Recently, we have characterized crosslinked species of minimal hammerheads involving the scissile linkage and domain II nucleobases G8 and G12. A C17•G8 crosslinked RNA retained catalytic activity, suggesting that at least some of these crosslinks may indicate close proximity in an active hammerhead fold that is substantially different from the crystallographic fold, in which C17 and G8 are 10−15 Å distant (*15*). Furthermore, we have used pH-activity relationships of hammerhead variants to propose a model for direct participation of G8 and G12 in a general acid−base mechanism for the hammerhead (*16*). Together, we believe that the accumulated evidence supports a model in which minimal

† This work is supported by Grant GM65552 to J.M.B. from the National Institutes of Health.

* To whom correspondence should be addressed. Department of Microbiology and Molecular Genetics, University of Vermont, 95 Carrigan Drive, 220B Stafford Hall, Burlington, VT 05405. Phone: (802) 656-8503. Fax: (802) 656-8749. E-mail: John.Burke@uvm.edu.

10.1021/bi052457x CCC: $33.50
Published on Web 05/18/2006

hammerheads fold to an inactive structure that dominates in solution and is similar to the crystallographic structures. This heavily populated ground-state fold coexists with a sparsely populated active fold that is formed transiently, but may be monitored through the C17•G8 crosslink described above.

Several groups have recently identified and characterized native hammerheads that have additional loop domains that interact and significantly increase activity under physiological conditions (low ionic strength), and it has been proposed that the native constructs may selectively stabilize the active fold (*17*−*20*). Here, we describe photocrosslinking studies designed to probe the folding of a native hammerhead derived from *Schistosoma mansoni* (*17*), with parallel experiments conducted using a minimal hammerhead whose connectivity facilitates analysis of domain II. We observe that the native and minimal constructs yield similar photocrosslinks between the cleavage site and putative active site nucleobases G8 and G12. Furthermore, the introduction of a novel photoreactive nucleobase, pyrrolocytidine, at cleavage site position C17 leads to the formation (in the presence of $[Co(NH_3)_6]^{3+}$) of a catalytically active crosslink to G12 in the native hammerhead. Analysis of the U-turn in native and minimal hammerheads suggests a rearrangement that positions the important and conserved nucleotide G5 near the cleavage site during folding to the active conformation. Finally, we present evidence for the induction of crosslinking between two nucleotides following the absorption of long-wavelength UV by a third nucleobase analogue. Together, these results indicate that the native hammerheads form an active fold similar to that of the minimal constructs and support a large-scale conformational rearrangement that is similar in both minimal and native hammerheads.

MATERIALS AND METHODS

RNA Preparation. All oligoribonucleotides were prepared by solid-phase synthesis using standard RNA phosphoramidite chemistry. Reagents were purchased from either Glen Research or Chemgenes. Following deprotection, RNA was purified by denaturing gel electrophoresis and reverse-phase HPLC,[1] as previously described (*21*).

Crosslinking Assays. The ribozyme−substrate complexes were reconstituted by incubating the 5′-^{32}P-end-labeled strand (approximately 200 nM for large-scale reactions estimated from RNA input of labeling) with an excess of the other strand (312.5 nM) in reaction buffer (50 mM MES pH 5.5 (for reaction in Mg^{2+}) or 50 mM HEPES pH 8.0 (for reaction in $[Co(NH_3)_6]^{3+}$), 100 mM NaCl, and 0.1 mM EDTA) for 2 min at 90 °C. Low pH in the Mg^{2+} reaction slows the cleavage to maximize crosslink yield. The higher pH of the $[Co(NH_3)_6]^{3+}$ crosslinking can be used because cleavage is slow, and $[Co(NH_3)_6]^{3+}$-mediated crosslinking is increased at high pH. The solutions were then allowed to equilibrate for 10 min at room temperature. Cleavage reactions of hammerhead α1 constructs were initiated by addition of 10 mM Mg^{2+} or 10 mM $[Co(NH_3)_6]^{3+}$, whereas cleavage reactions of the *S. mansoni* hammerhead were initiated by addition of 1 mM Mg^{2+} or 10 mM $[Co(NH_3)_6]^{3+}$. Different Mg^{2+} concentrations were used with the two ribozymes to obtain similar cleavage rates so that less than half the substrate would be cleaved during the 5-min irradiation. Reactions were immediately irradiated at 312 nm for 5 min, using a hand-held lamp from International Biotechnologies, Inc. model VL-6M, power 12 W. Samples containing pyrrolocytidine were irradiated at 365 nm for 5 min with a UVP model UVL-56 hand-held lamp, 115 V, 50/60 Hz, 0.16 amps, and crosslinked species were isolated as described by Pinard et al. (*21*).

Mapping of the Crosslinked Species. Crosslinking sites were mapped as described by Pinard et al. (*22*).

Activity Assays of Crosslinked Ribozyme−*Substrate Complex.* The hammerhead α1 crosslinked species were incubated in reaction buffer (50 mM HEPES, pH 8.0, and 0.1 mM ATA). ATA (aurintricarboxylic acid) was added to inhibit traces of protein ribonuclease. The samples were allowed to equilibrate in this buffer for 10 min at 37 °C. Cleavage reactions were initiated by the addition of 10 mM Mg^{2+} and incubated at 37 °C for 2 h. The crosslinked species obtained in *S. mansoni* hammerhead were incubated in reaction buffer (50 mM HEPES, pH 8.0, 100 mM NaCl, 0.1 mM EDTA, and 0.1 mM ATA) for 2 min at 70 °C. The solutions were then allowed to equilibrate for 10 min at 37 °C. Cleavage reactions were initiated by the addition of 1 mM Mg^{2+} and incubated at 37 °C for 2 h. Pyrrolocytidine crosslinks were incubated in reaction buffer (50 mM Tris-Hcl, pH 7.2, 0.1 mM EDTA, 0.1 mM ATA, and 100 mM NaCl) for 2 min at 70 °C. The solutions were then allowed to equilibrate for 10 min at 25 °C. Cleavage reaction were initiated with either 1 mM $MgCl_2$ or 1.2 M LiCl and incubated at 25 °C for 2 h. All reactions were stopped by the addition of 3 vol of a solution containing 90% formamide and 1 mM EDTA and loaded directly onto a denaturing 20% polyacrylamide gel.

RESULTS

Conformations of Domain II in Active and Ground-State Folds in a Minimal Hammerhead. Domain II contains several functional groups that are essential for activity. In the crystal structure, domain II consists of two helices flanking four noncanonical base pairs, including two stacked sugar-edge/Hoogsteen (sheared) base pairs, G8•A13 and G12•A9 (Figure 1). This motif is common at the junction of coaxially stacked helices and is thought to maintain the overall axis of the helical segment (*23*, *24*). Because intrastrand photocrosslinks are extremely difficult to isolate and analyze, we investigated the conformations of domain II in the background of hammerhead α1, in which the 5′ and 3′ regions of domain II are on separate strands (Figure 1), using variants containing photoreactive nucleobases at sites of interest.

Ribozyme−substrate complexes were synthesized containing 6-thioguanosine (6sG) at positions 8 and 12 of hammerhead α1 (*25*). The modifications decreased the cleavage rates slightly (i.e., after 60 min, the extent of cleavage for 6sG8 was 30% that of wild-type, and 6sG12's was 15% that of wild-type). Crosslinks were obtained following 312 nm photoirradiation of RNA molecules folded in the presence of 10 mM Mg^{2+} or 10 mM $[Co(NH_3)_6]^{3+}$. As expected from

[1] Abbreviations: ATA, aurintricarboxylic acid; 4sU, 4-thiouridine; 6sdG, 6-thio-2′-deoxyguanosine; 6sG, 6-thioguanosine; EDTA, ethylenediaminetetraacetic acid; HEPES, *N*-(2-hydroxyethyl)piperazine-*N*′-(2-ethane sulfonic acid); HPLC, high-performance liquid chromatography; MES, 2-(*N*-morpholino)ethanesulfonic acid; NMR, nuclear magnetic resonance; Tris, Tris(hydroxymethyl)aminomethane.

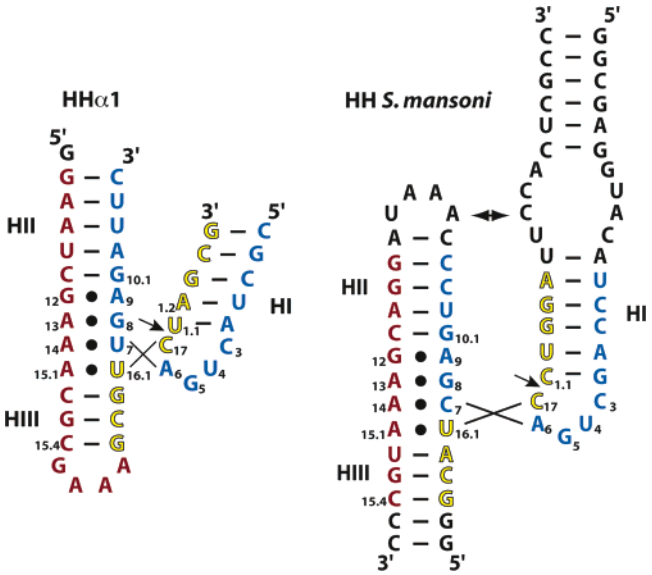

FIGURE 1: The hammerhead−ribozyme substrate complex. Secondary structures of the hammerhead ribozyme constructs used in this study. Residues corresponding to the substrate are shown in yellow. Residues constituting the ribozyme strand are colored in red (long strand for HHα1) and blue (short strand for HHα1). Residues from the conserved core are annotated, and the cleavage site is indicated by an arrow.

Table 1: Summary of Photocrosslinking Results in Hammerhead α1

long strand nt	XL agent	XL site	metal	D crystal[a]
12	6-thio-dG	G8	Mg^{2+}	7.34
12	6-thio-dG	G8	$Co(NH_3)_6^{3+}$	7.34
12	6-thio-G	G8	Mg^{2+}	7.34
12	6-thio-G	G8	$Co(NH_3)_6^{3+}$	7.34
13	2,6-diAP	G8/A9	$Co(NH_3)_6^{3+}$	8.20/5.17
13	2,6-diAP	G10.1	$Co(NH_3)_6^{3+}$	7.18
15.1	2,6-diAP	A14-G8	$Co(NH_3)_6^{3+}$	7.41
short strand nt	**XL agent**	**XL site**	**metal**	**D crystal[a]**
5	6-thio-G	U1.1	Mg^{2+}	11.62
5	6-thio-G	15.4/GNRA	Mg^{2+}	9.78
5	6-thio-G	C17	$Co(NH_3)_6^{3+}$	8.02
6	2,6-diAP	15.3	$Co(NH_3)_6^{3+}$	8.90
8	6-thio-dG	G12	Mg^{2+}	7.34
8	6-thio-dG	G12	$Co(NH_3)_6^{3+}$	7.34
8	6-thio-G	C17/U1.1	Mg^{2+}	13.55/16.37
8	6-thio-G	G12	$Co(NH_3)_6^{3+}$	7.34

[a] Distance measured in Å between glycosyl nitrogen atoms.

G8−G12 stacking in the crystal structure, 6sG12 resulted in crosslinks to G8, and 6sG8 yielded the reciprocal crosslink to G12. Identical results were obtained when 2′-deoxy-6-thioguanosine (d6sG) was used. We also isolated and characterized a crosslink from 6sG8 to cleavage site nucleobase U1.1 (Table 1). This latter crosslink is consistent with previous work in which we observed multiple crosslinks between G8, G12, and the cleavage site nucleobases (*15*). Attempts to obtain a reciprocal crosslink to domain II using 4-thiouridine (4sU) at substrate position 1.1 were unsuccessful; the 4sU substitution was inhibitory. None of the crosslinks mentioned above showed cleavage activity (data not shown). Together, these results are consistent with a two-state folding model implied by previous findings (*15*, *16*) in which the hammerhead partitions between an inactive ground state (giving rise to the G8−G12 crosslinks) and an active fold where G8 and G12 interact with the cleavage site.

Table 2: Summary of Photocrosslinking Results in *S. mansoni* Native Hammerhead

ribozyme nt	XL agent	XL site	metal	D crystal[a]
U4	4-thio-U	C1.1	Mg^{2+}	7.86
G5	6-thio-G	C1.1[b]	Mg^{2+}	11.62
G5	6-thio-G	G12-C17	Mg^{2+}	19.33
U7	4-thio-U	Kiss-loops	$Co(NH_3)_6^{3+}$	-
G8	6-thio-G	C1.1[b]	Mg^{2+}	16.37
G12	6-thio-G	C17	Mg^{2+}	19.33
G12	6-thio-G	G8/U1.1	Mg^{2+}	16.37
substrate nt	**XL agent**	**XL site**	**metal**	**D crystal[a]**
U16.1	4-thio-U	U4	Mg^{2+}	10.89
U16.1	4-thio-U	A13/A14	Mg^{2+}	15.93/13.48
U16.1	4-thio-U	G5-C1.1	Mg^{2+}	11.62
C17	pyC	G8	$Co(NH_3)_6^{3+}$	13.55
C17	pyC	G12[c]	$Co(NH_3)_6^{3+}$	19.33

[a] Distance measured in Å between glycosyl nitrogen atoms. [b] The cutoff of this crosslink is a mixture of G5 and G8. [c] Crosslink retained catalytic activity.

Investigation of the stacking interactions of A9 and A13 proved to be more difficult, at least in part because the available crosslinking agents, 2AP and diAP, are not ideal structural homologues of adenosine, and in the crystal structure, the Hoogsteen faces of A9 and A13 form multiple inferred hydrogen bonds with the sugar edges and riboses of G12 and G8, respectively. Complexes were generated containing 2,6-diaminopurine (diAP) at positions 9 and 13. The diAP9 substitution was severely inhibitory, while diAP13 showed normal activity (data not shown); the diAP9 variant was not pursued further. Long-wavelength (312 nm) irradiation of the diAP13 variant in the presence of $[Co(NH_3)_6]^{3+}$ generated two crosslinks that could be separated by electrophoresis (Table 1). One was diAP13 crosslinked to a mixture of G8 and A9, and had no residual catalytic activity. The second crosslink is from diAP13 to G10.1, which also failed to show catalytic activity. Both could be derived from the ground-state fold, since A13 is positioned close to these residues in the crystal structure.

Conformations of the U-Turn in a Minimal Hammerhead. Crystal structures show that domain I contains a U-turn motif involving residues 3−6 (Figure 1), but the structure does not rationalize the requirement for many functional groups within the turn, especially those on G5. Previously, we reported crosslinking experiments from 6sdG5 and 8-Br-G5 to the cleavage site nucleobase at position 1.1 in hammerhead 16 (*15*). Because the 2′-OH of G5 is important for folding to an active structure (*26*) and 8-Br-G strongly prefers a syn conformation (*27*), we extended this analysis using the newly available 6sG at position 5 in hammerhead α1. Consistent with the previous findings, a crosslink was mapped from 6sG5 to U1.1. Additional crosslinks were mapped from 6sG5 to C15.4 and to the tetraloop capping helix III (Table 1). Note that the latter crosslinks would not have been detected in the previous study (*15*) due to differences in strand connectivity in the hammerhead 16 construct used in that work. When 10 mM $[Co(NH_3)_6]^{3+}$ was used instead of 10 mM Mg^{2+}, crosslinks were identified that connected 6sG5 to C17 and diAP6 to G15.3 (Table 1). None of the 6sG5 or diAP6 crosslinks were observed to retain catalytic activity.

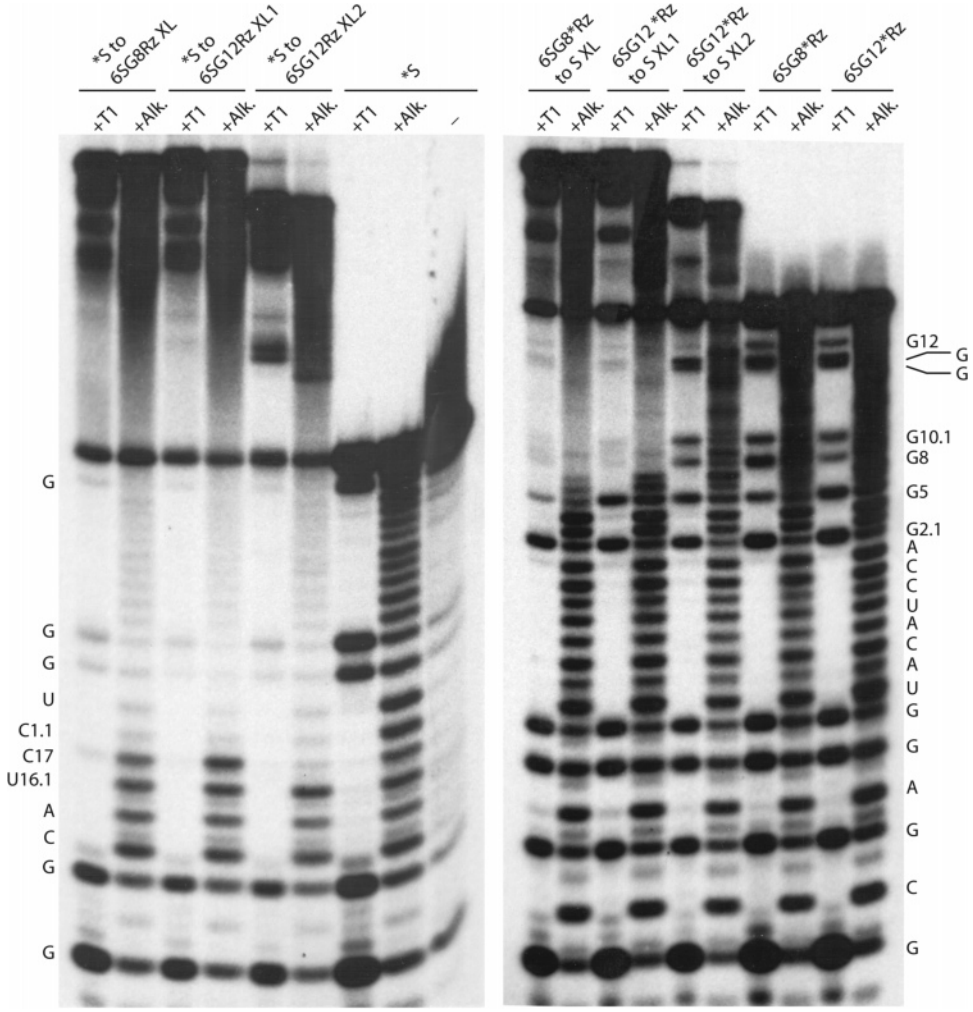

FIGURE 2: Sequencing of 6sG8 and 6sG12 crosslinks in the *S. mansoni* native ribozyme. The crosslinked sites were mapped by limited alkaline hydrolysis (Alk) and partial digestion with RNAse T1 (T1). The species consisting of 5′-^{32}P-end-labeled substrate crosslinked to 6sG8− or 6sG12−ribozyme strand (*S to 6sG8Rz-, 6sG12Rz XL), and the end-labeled substrate control (*S) are on the left. The species consisting of 5′-^{32}P-end-labeled 6sG8− or 6sG12−ribozyme strand crosslinked to substrate (S to 6sG8*Rz-, 6sG12*Rz XL), and the end-labeled 6sG8*Rz-, 6sG12*Rz controls are on the right. Sites of T1-induced cleavages are indicated by the numbered guanosine. Note that a 6sG12 yields the expected 6sG12•C17 crosslink, plus a G8•C1.1 crosslink, and 6sG8 gives a mixed crosslink (partial cutoff at G5) to C1.1.

These observations suggest that the functionally important nucleobase G5 can interact with two different sites in the hammerhead, the cleavage site and the distal segment of helix III. These sites are approximately 12 and 10 Å distant from G5 in the crystallographic structures. We infer that the hammerhead folds that give rise to these crosslinks are different from one another and different from the crystal structure. These observations suggest that the U-turn of the minimal hammerheads may be highly flexible and/or dynamic. One or both sets of interactions could represent an inactive conformation, but the biochemical importance of G5 implies that it makes interactions in the active fold.

G8 and G12 Interact with the Cleavage Site of a Native Hammerhead. We wished to determine if the interaction between G8, G12, and the substrate cleavage site was a general feature of hammerhead ribozymes or was idiosyncratic to minimal constructs. Therefore, we replaced G8 and G12 of the native *S. mansoni* hammerhead with 6sG and conducted photocrosslinking analyses similar to those described above. In this native hammerhead, neither 6sG8 nor 6sG12 was observed to reduce catalytic activity significantly (after 30 min incubation, cleavage extent by the 6sG8 and 6sG12 ribozymes was at least 80% that of the unmodified ribozyme), and both yielded crosslinks to the substrate cleavage site analogous to those seen with the minimal constructs—6sG8 crosslinked to C1.1 and 6sG12 crosslinked to C17 (Table 2, Figure 2).

Unexpectedly, we mapped crosslinks from these variant RNA molecules that did not involve the modified nucleobase. The 6sG12 RNA generated a G8•C1.1 crosslink, and the 6sG8 RNA generated a G5•C1.1 crosslink, all in addition to the expected crosslinks (Figure 2). The mechanism through which a photoreactive nucleobase induces crosslinking between two other nucleobases is intriguing but unknown. However, it may be that close proximity of the three nucleobases facilitates the phenomenon. Alternatively, the photoactivation might be transferred through a free radical reaction.

Pyrrolocytidine (pyC), a fluorescent nucleotide analogue (*28*), was introduced at the substrate cleavage site (pyC17) and was found to be efficiently cleaved by the hammerhead (Fay, M., and Burke, J., unpublished work). Exceptionally high yields of photocrosslinks were obtained when ribozyme−substrate complexes containing pyC17 were ir-

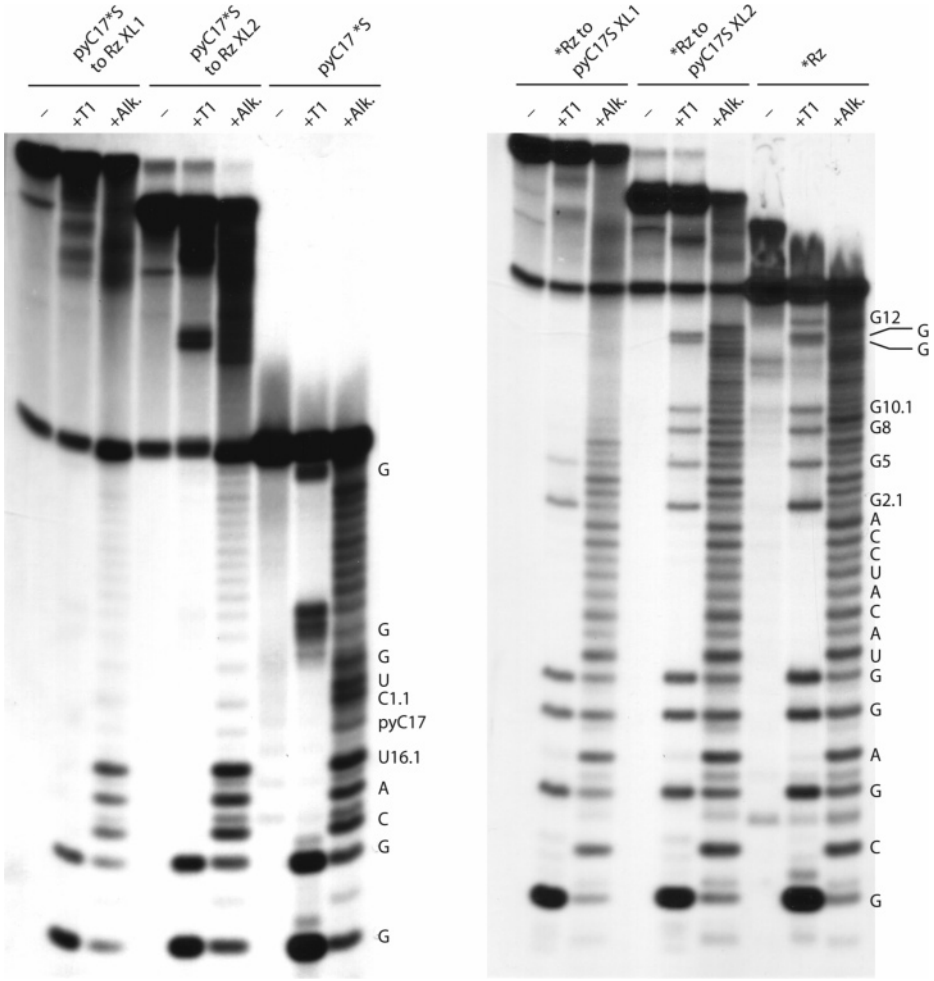

FIGURE 3: Sequencing of cobalt hexaammine-induced pyrroloC17 crosslinks in the *S. mansoni* native hammerhead. The crosslinked sites were mapped by limited alkaline hydrolysis (Alk) and partial digestion with RNAse T1 (T1). Untreated crosslinks are also shown (−). The species consisting of 5′-^{32}P-end-labeled pyrrolocytidine substrate crosslinked to ribozyme strand (pyC17*S to Rz XL1−2) and the end-labeled substrate control (pyC17*S) are on the left. The species consisting of 5′-^{32}P-end-labeled ribozyme strand crosslinked to substrate (*Rz to pyC17S XL1−2) and the 5′-^{32}P-end-labeled ribozyme strand control are on the right. Sites of T1-induced cleavages are indicated by the numbered guanosine.

radiated in solutions containing $[Co(NH_3)_6]^{3+}$, and the crosslinks obtained were mapped from pyC17 to G8 and to G12 (Table 2, Figure 3). Furthermore, the pyC17•G12 crosslinked RNA is weakly but detectably catalytically active when examined in the presence of either Mg^{2+} or Li^{+} (Figure 4). These results are consistent with our proposal that the cleavage site approaches nucleobases G8 and G12 during accession of the catalytic conformation (*15*, *16*).

Conformations of the U-Turn in a Native Hammerhead. To investigate a possible structural rearrangement in the U-turn of the native hammerhead, we introduced 6sG at position 5, as well as 4-thiouridine (4sU) at positions 4 and 7, and conducted photocrosslinking analysis in solutions containing Mg^{2+} (Table 2). None of the modifications interfered dramatically with catalytic activity (the extent of cleavage after 30 min incubation by 6sG5 ribozyme was ∼80% that of unmodified ribozyme). The 6sG5 RNA generated crosslinks from both position 5 and G8 to C1.1, and also induced a C17•G12 crosslink (Figure 5). The 4sU4 RNA gave crosslinks from position 4 to C1.1 (Table 2). No crosslinks were obtained from 4sU7, although a crosslink between the 'kissing loops' of the native ribozyme was seen (data not shown). Attempts to obtain crosslinks from RNA containing pyC7 were unsuccessful.

Because U16.1 is located adjacent to the U-turn, we introduced 4sU at this position to map its proximity to nucleobases within the U-turn. In contrast to results that would be anticipated from the crystal structure, where G5 and A6 are closely packed with U16.1, we obtained crosslinks to U4 and A14 (Table 2). In addition, 4sU16.1 generated a crosslink between residues G5 and C1.1 (Table 2). None of the crosslinks possessed detectable catalytic activity.

DISCUSSION

Active Structure of Native Hammerheads. Results of the present studies of domain II in native and minimal hammerheads are in agreement with our model for formation of an active site in which G8 and G12 function in general acid−base catalysis (*16*), characterized by stacking of G8 and G12 upon the cleavage site nucleobases C17 and C or U at position 1.1 (*15*), through a conformational change from the ground state (crystallographic) structure. Use of hammerhead α1 facilitated isolation of crosslinks between the two strands of the ribozyme in the region of helix II and helix III, but aside from that, no significant differences were observed when the minimal versus native hammerheads were examined, suggesting that the structure of the proposed active site

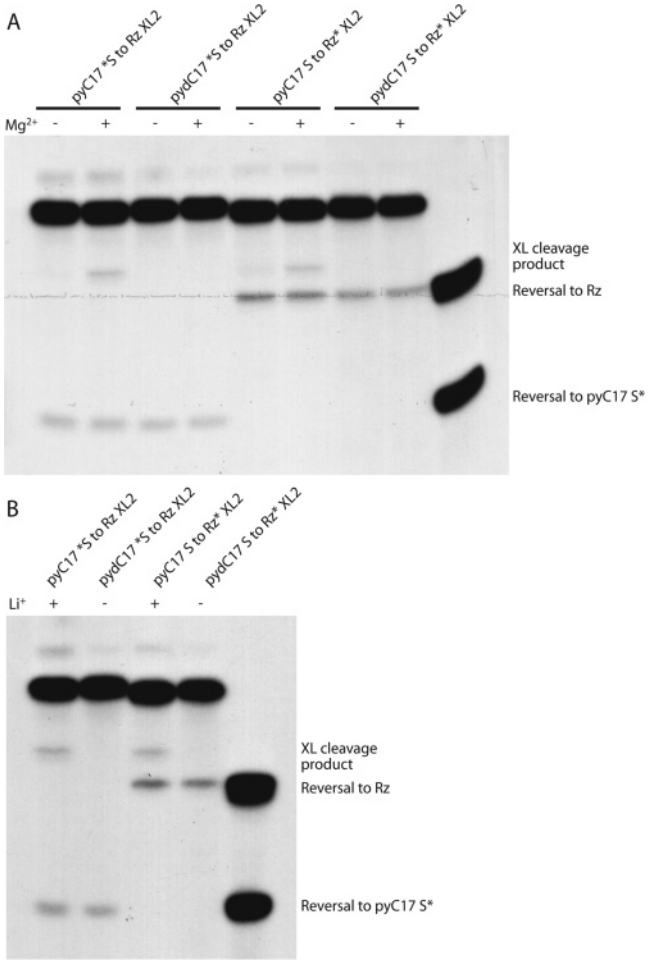

FIGURE 4: Activity assay of cobalt hexaammine-induced pyrroloC17 crosslink. The species consisting of 5′-^{32}P-end-labeled pyrrolocytidine substrate crosslinked to ribozyme strand (pyC17*S to Rz XL2) and 5′-^{32}P-end-labeled 2′-deoxypyrrolocytidine noncleavable substrate crosslinked to ribozyme strand (pydC17*S to Rz XL2) are on the left, and 5′-^{32}P-end-labeled ribozyme strand crosslinked to pyC17 substrate (pyC17S to Rz* XL2) and 5′-^{32}P-end-labeled ribozyme strand crosslinked to pydC17 substrate (pydC17S to Rz* XL2) are on the right. Species were incubated in the absence or presence of magnesium (A) or lithium (B). The 5′-^{32}P-end-labeled crosslink cleavage produced is indicated, as well as the reversal to 5′-^{32}P-end-labeled ribozyme and 5′-^{32}P-end-labeled py(d)C17 substrate products. The crosslinked species, if cleaved, would lose a 16-nt 3′ cleavage product, and the 7-nt 5′ cleavage product would remain covalently attached to the ribozyme. Thus, the crosslink cleavage product, whether 5′-labeled on substrate or ribozyme, migrates identically.

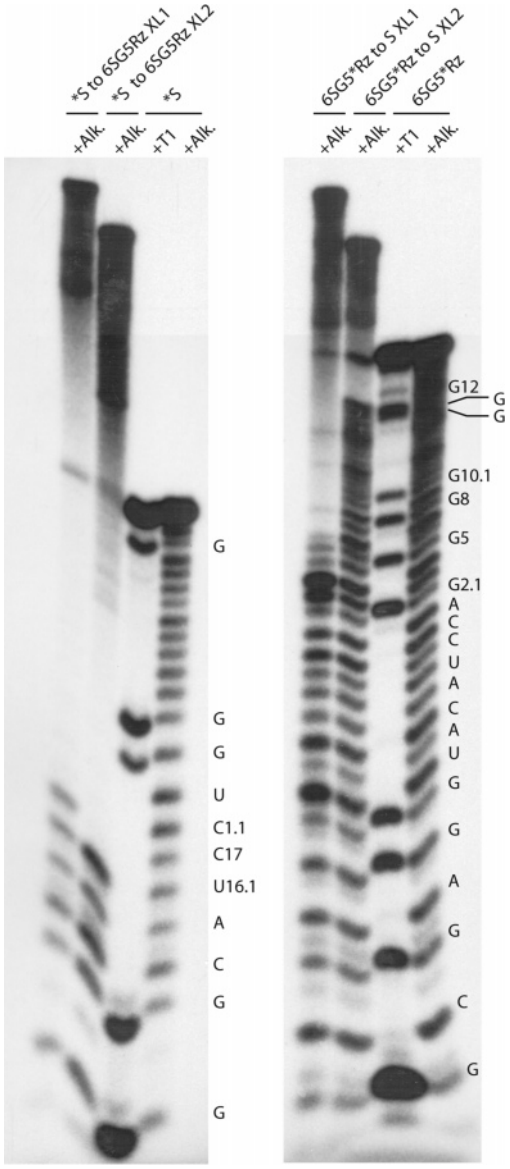

FIGURE 5: Sequencing of 6sG5 crosslinks in the *S. mansoni* native ribozyme. The crosslinked sites were mapped by limited alkaline hydrolysis (Alk) and partial digestion with RNAse T1 (T1). The species consisting of 5′-^{32}P-end-labeled substrate crosslinked to 6sG5 ribozyme strand (*S to 6sG5Rz XL 1−2) and the end-labeled substrate control (*S) are on the left. The species consisting of 5′-^{32}P-end-labeled 6sG5 ribozyme strand crosslinked to substrate (S to 6sG5*Rz XL 1−2) and the 5′-^{32}P-end-labeled 6sG5*Rz control are on the right. Sites of T1-induced cleavages are indicated by the numbered guanosine.

is similar in each construct studied (minimal hammerheads 16 and α1, and the native *S. mansoni* ribozyme) (Figure 6). The native hammerheads did not produce high crosslinking yields compared to the minimal constructs, perhaps because their stabilized folding constrains stacking relationships explored by the molecule.

G5 and the U-Turn. The finding that 6sG5 can be crosslinked to the cleavage site and to distal regions of helix III, both of which are significantly distant from G5 in the crystal structure, supports the notion that the U-turn has significant conformational flexibility (*29*). In a minimal ribozyme, the helix connected to the U-turn (helix I) has been shown to explore a large conformational space and to move closer to helix II with increasing concentrations of magnesium ions (*26*). The role of G5 in hammerhead catalysis remains unclear; pH-activity studies using modified nucleobases argue against a direct function in acid−base catalysis, but other essential roles, for example, facilitating the conformational change to the active structure, are possible. A metal ion-dependent rearrangement has been proposed based on experiments done in the presence of terbium ions. Tb^{3+} inhibits the cleavage reaction, and a terbium-binding site has been identified in the vicinity of G5 (*30*, *31*). Inhibition has been proposed to result from tight binding of Tb^{3+} interfering with a Mg^{2+}-dependent conformational change (*32*). This proposal is consistent with our observation that none of the G5-crosslinked hammerheads retained cleavage activity. Our data confirm that the formation of a crosslink between nucleobases G5 and N1.1 can be observed in three different

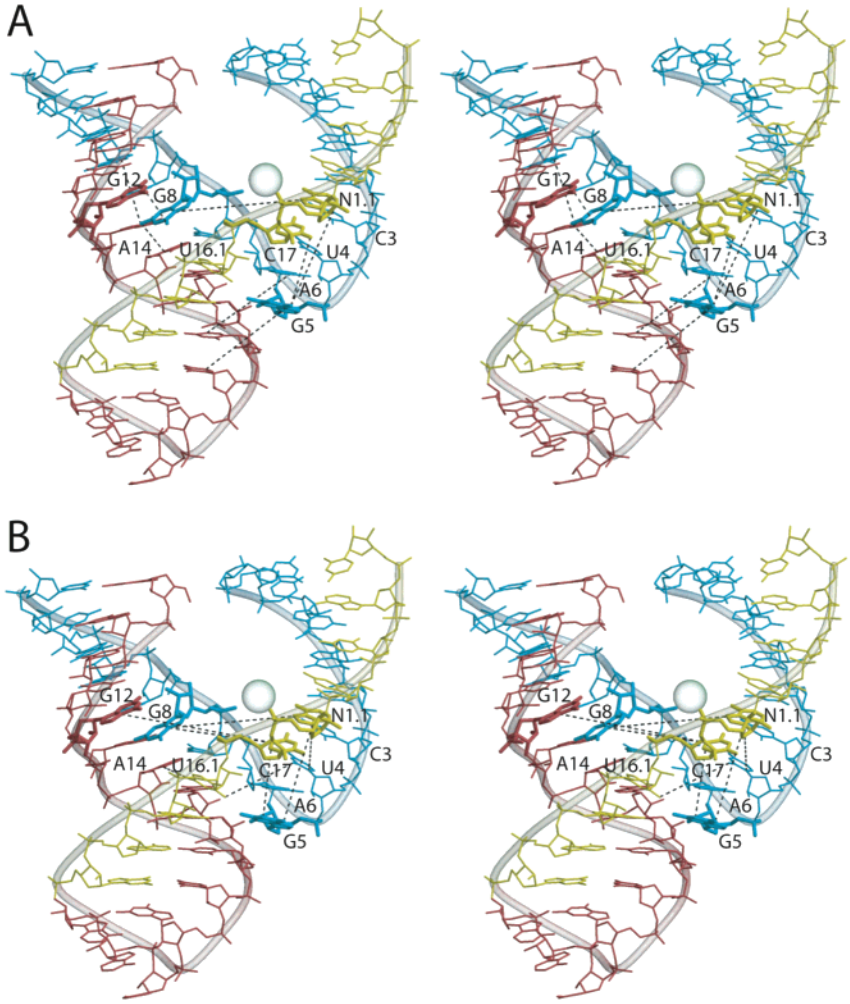

FIGURE 6: Summary of crosslinks. (A) Crosslinks obtained in hammerhead α1; (B) crosslinks obtained in the *S. mansoni* native hammerhead, depicted in the crystal (ground state) structure of the minimal hammerhead ribozyme (*4*).

hammerheads, including a native construct, and consequently does not represent an artifact characteristic of minimal ribozymes.

Trans-Photoactivation by Thio-Modified Nucleobases. The most surprising result of this work is that the irradiation of native hammerheads containing a single photoreactive nucleobase was observed to induce crosslinking between two other nucleobases. This was observed in the case of 4sU16.1, which induced a G5•C1.1 crosslink, 6sG5, which induced a G12•C17 crosslink, as well as 6-thioG8, which induced a G5•C1.1, and 6-thioG12, which induced a G8•C1.1 crosslink (Table 2, Figure 2, Figure 5). These results could suggest a close three-dimensional proximity of the three bases. Two different mechanisms can be envisioned. First, the thio modification could result in a change in the folded structure such that the two crosslinked bases become more closely stacked on one another. Second, an energy transfer or electron-transfer event could take place to or from the electronic excited state resulting from photon absorption of the modified nucleobase into another base, leading to crosslinking. The fact that we observed these events in ribozymes with different modifications leads us to favor the second hypothesis. Interestingly, we have never observed such cross-activation from nucleotide analogues in minimal hammerhead ribozymes in magnesium. The stabilized folded structure of the native ribozyme may facilitate cross-reaction between closely oriented residues, especially guanosines. Our results suggest that the native hammerhead might form a more compact active fold than minimal hammerheads. Alternatively, these observations can be due to a long-lived folding intermediate in which G5, G8, and G12 are in proximity to one another.

Summary. In summary, we have used an experimental approach combining nucleotide substitution and photochemical crosslinking to examine the structure of the hammerhead ribozyme in solution, comparing minimal and native constructs. Our results support a model in which both hammerheads partition between two folds—an inactive ground state similar to the crystallographic structures and an active fold characterized by interactions between putative catalytic nucleobases G8 and G12 and the substrate cleavage site. Accessing the active fold would involve movement of the cleavable linkage close to the metal binding site at residues A9 and G10.1, as suggested by Wang et al. (*10*), a distance of nearly 20 Å in the crystal structure (*33*). That movement would necessitate a change in the structure of the "U-turn" region around G5, as suggested here by the crosslinks obtained from 6sG5. Information gleaned from the active fold of the native ribozyme indicates that its structure is very similar to that of the active fold of the minimal hammerhead, and provides additional information concerning the conformation of the U-turn and, particularly, G5.

ACKNOWLEDGMENT

We thank Kenneth Hampel, Michael Fay, Christina Kraemer-Chant, and Joonhee Han for helpful discussions and insights. Additionally, we thank Michael Fay for synthesis of RNA as well as Anne MacLeod for work on the manuscript.

REFERENCES

1. Pley, H. W., Flaherty, K. M., and McKay, D. B. (1994) Three-dimensional structure of a hammerhead ribozyme, *Nature 372*, 68−74.
2. Scott, W. G., Finch, J. T., and Klug, A. (1995) The crystal structure of an all-RNA hammerhead ribozyme: a proposed mechanism for RNA catalytic cleavage, *Cell 81*, 991−1002.
3. Dunham, C. M., Murray, J. B., and Scott, W. G. (2003) A helical twist-induced conformational switch activates cleavage in the hammerhead ribozyme, *J. Mol. Biol. 332*, 327−336.
4. Murray, J. B., Dunham, C. M., and Scott, W. G. (2002) A pH-dependent conformational change, rather than the chemical step, appears to be rate-limiting in the hammerhead ribozyme cleavage reaction, *J. Mol. Biol. 315*, 121−130.
5. Soukup, G. A., and Breaker, R. R. (1999) Relationship between internucleotide linkage geometry and the stability of RNA, *RNA 5*, 1308−1325.
6. Murray, J. B., Seyhan, A. A., Walter, N. G., Burke, J. M., and Scott, W. G. (1998) The hammerhead, hairpin and VS ribozymes are catalytically proficient in monovalent cations alone, *Chem. Biol. 5*, 587−595.
7. O'Rear, J. L., Wang, S., Feig, A. L., Beigelman, L., Uhlenbeck, O. C., and Herschlag, D. (2001) Comparison of the hammerhead cleavage reactions stimulated by monovalent and divalent cations, *RNA 7*, 537−545.
8. Zhou, J. M., Zhou, D. M., Takagi, Y., Kasai, Y., Inoue, A., Baba, T., and Taira, K. (2002) Existence of efficient divalent metal ion-catalyzed and inefficient divalent metal ion-independent channels in reactions catalyzed by a hammerhead ribozyme, *Nucleic Acids Res. 30*, 2374−2382.
9. Blount, K. F., and Uhlenbeck, O. C. (2005) The structure−function dilemma of the hammerhead ribozyme, *Annu. Rev. Biophys. Biomol. Struct. 34*, 415−440.
10. Wang, S., Karbstein, K., Peracchi, A., Beigelman, L., and Herschlag, D. (1999) Identification of the hammerhead ribozyme metal ion binding site responsible for rescue of the deleterious effect of a cleavage site phosphorothioate, *Biochemistry 38*, 14363−14378.
11. Derrick, W. B., Greef, C. H., Caruthers, M. H., and Uhlenbeck, O. C. (2000) Hammerhead cleavage of the phosphorodithioate linkage, *Biochemistry 39*, 4947−4954.
12. Wedekind, J. E., and McKay, D. B. (1998) Crystallographic structures of the hammerhead ribozyme: relationship to ribozyme folding and catalysis, *Annu. Rev. Biophys. Biomol. Struct. 27*, 475−502.
13. Blount, K. F., Grover, N. L., Mokler, V., Beigelman, L., and Uhlenbeck, O. C. (2002) Steric interference modification of the hammerhead ribozyme, *Chem. Biol. 9*, 1009−1016.
14. Hampel, K. J., and Burke, J. M. (2003) Solvent protection of the hammerhead ribozyme in the ground state: evidence for a cation-assisted conformational change leading to catalysis, *Biochemistry 42*, 4421−4429.
15. Heckman, J. E., Lambert, D., and Burke, J. M. (2005) Photo-crosslinking detects a compact, active structure of the hammerhead ribozyme, *Biochemistry 44*, 4148−4156.
16. Han, J., and Burke, J. M. (2005) Model for general acid-base catalysis by the hammerhead ribozyme: pH-activity relationships of G8 and G12 variants at the putative active site, *Biochemistry 44*, 7864−7870.
17. Canny, M. D., Jucker, F. M., Kellogg, E., Khvorova, A., Jayasena, S. D., and Pardi, A. (2004) Fast cleavage kinetics of a natural hammerhead ribozyme, *J. Am. Chem. Soc. 126*, 10848−10849.
18. Gago, S., De la Pena, M., and Flores, R. (2005) A kissing-loop interaction in a hammerhead viroid RNA critical for its in vitro folding and in vivo viability, *RNA*, 1073−1083.
19. Khvorova, A., Lescoute, A., Westhof, E., and Jayasena, S. D. (2003) Sequence elements outside the hammerhead ribozyme catalytic core enable intracellular activity, *Nat. Struct. Biol. 10*, 708−712.
20. Osborne, E. M., Schaak, J. E., and Derose, V. J. (2005) Characterization of a native hammerhead ribozyme derived from schistosomes, *RNA 11*, 187−196.
21. Pinard, R., Lambert, D., Heckman, J. E., Esteban, J. A., Gundlach, C. W., IV, Hampel, K. J., Glick, G. D., Walter, N. G., Major, F., and Burke, J. M. (2001) The hairpin ribozyme substrate binding-domain: a highly constrained D-shaped conformation, *J. Mol. Biol. 307*, 51−65.
22. Pinard, R., Heckman, J. E., and Burke, J. M. (1999) Alignment of the two domains of the hairpin ribozyme-substrate complex defined by interdomain photoaffinity crosslinking, *J. Mol. Biol. 287*, 239−251.
23. Gao, Y. G., Robinson, H., Sanishvili, R., Joachimiak, A., and Wang, A. H. (1999) Structure and recognition of sheared tandem G•A base pairs associated with human centromere DNA sequence at atomic resolution, *Biochemistry 38*, 16452−16460.
24. Elgavish, T., Cannone, J. J., Lee, J. C., Harvey, S. C., and Gutell, R. R. (2001) AA.AG@helix.ends: A:A and A:G base-pairs at the ends of 16 S and 23 S rRNA helices, *J. Mol. Biol. 310*, 735−753.
25. Clouet-d'Orval, B., and Uhlenbeck, O. C. (1997) Hammerhead ribozymes with a faster cleavage rate, *Biochemistry 36*, 9087−9092.
26. Bassi, G. S., Mollegaard, N. E., Murchie, A. I., and Lilley, D. M. (1999) RNA folding and misfolding of the hammerhead ribozyme, *Biochemistry 38*, 3345−3354.
27. Proctor, D. J., Kierzek, E., Kierzek, R., and Bevilacqua, P. C. (2003) Restricting the conformational heterogeneity of RNA by specific incorporation of 8-bromoguanosine, *J. Am. Chem. Soc. 125*, 2390−2391.
28. Berry, D. A., Jung, K. Y., Wise, D. S., Sercel, A. D., Pearson, W. H., Mackie, H., Randolph, J. B., and Somers, R. L. (2004) Pyrrolo-dC and pyrrolo-C: fluorescent analogs of cytidine and 2′-deoxycytidine for the study of oligonucleotides, *Tetrahedron Lett. 45*, 2457−2461.
29. Simorre, J. P., Legault, P., Baidya, N., Uhlenbeck, O. C., Maloney, L., Wincott, F., Usman, N., Beigelman, L., and Pardi, A. (1998) Structural variation induced by different nucleotides at the cleavage site of the hammerhead ribozyme, *Biochemistry 37*, 4034−4044.
30. Lott, W. B., Pontius, B. W., and von Hippel, P. H. (1998) A two-metal ion mechanism operates in the hammerhead ribozyme-mediated cleavage of an RNA substrate, *Proc. Natl. Acad. Sci. U.S.A. 95*, 542−547.
31. Feig, A. L., Scott, W. G., and Uhlenbeck, O. C. (1998) Inhibition of the hammerhead ribozyme cleavage reaction by site- specific binding of Tb, *Science 279*, 81−84.
32. Feig, A. L., Panek, M., Horrocks, W. D., Jr., and Uhlenbeck, O. C. (1999) Probing the binding of Tb(III) and Eu(III) to the hammerhead ribozyme using luminescence spectroscopy, *Chem. Biol. 6*, 801−810.
33. Murray, J. B., and Scott, W. G. (2000) Does a single metal ion bridge the A-9 and scissile phosphate groups in the catalytically active hammerhead ribozyme structure? *J. Mol. Biol. 296*, 33−41.

BI052457X